ISSN No. 2321-2705 | DOI: 10.51244/IJRSI |Volume XIII Issue XI November 2026

Griffiths Electromagnetic Bowl Cutter (GEMBC): Field-Governed Comminution and Emulsification Architecture for High-Integrity Industrial Food Processing

Wayne Griffiths

Founder and President, AEMS LLC · Griffiths Canon Research Group

DOI: https://doi.org/10.51244/IJRSI.2026.1311000027

Received: 04 November 2026; Accepted: 09 November 2026; Published: 20 November 2026

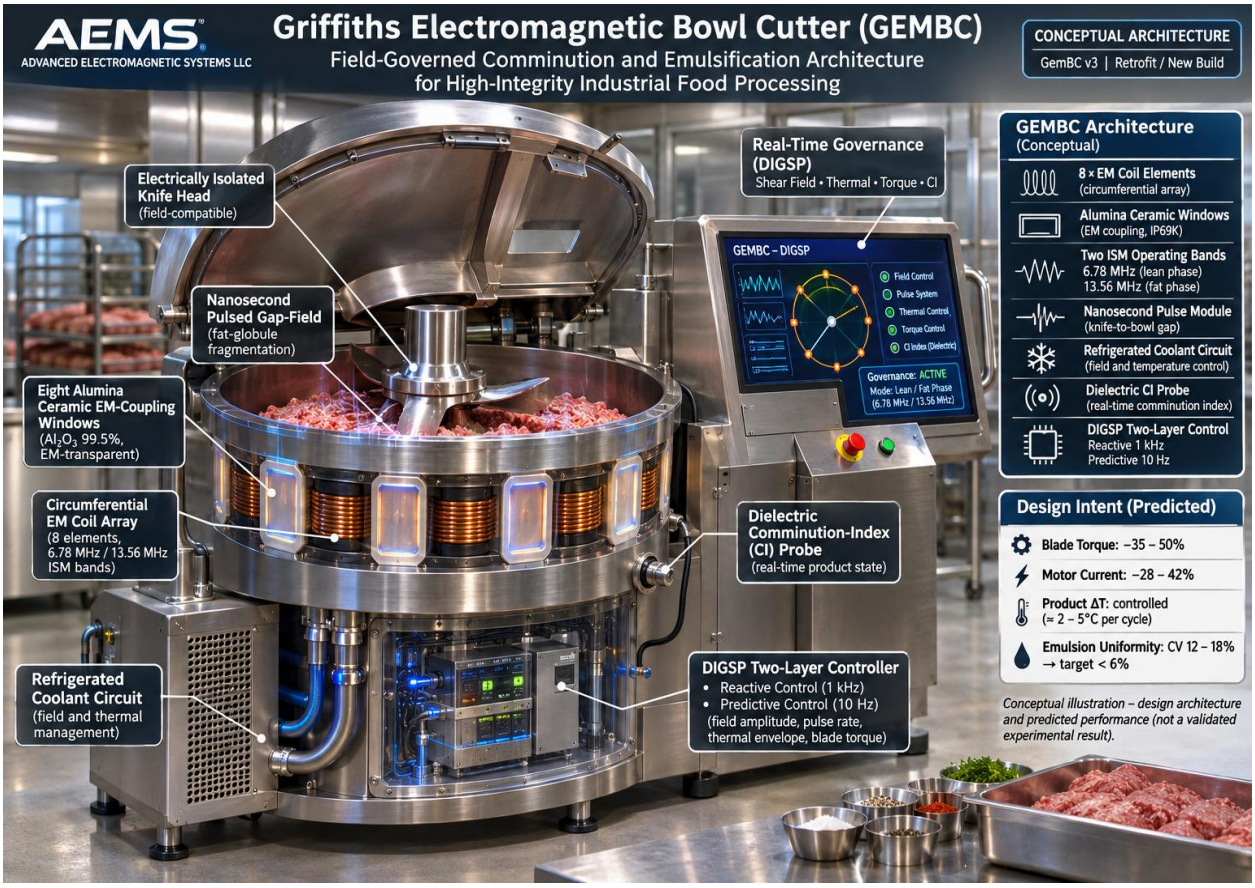

FIGURE 1. AEMS L500 series bowl cutter, the conventional form factor targeted by GEMBC. The retrofit introduces eight alumina ceramic EM-coupling windows machined into the outer 316L shell, a circumferential coil array (8 elements, GaN/SiC PMU-driven), a nanosecond pulse module with knife-to-bowl gap electrodes, a refrigerated coolant circuit, a twelve-point thermal sensor ring, and the DIGSP two-layer controller, all within the existing frame footprint, with the knife head electrically insulated from the bowl.

EXECUTIVE SUMMARY

The Griffiths Electromagnetic Bowl Cutter (GEMBC) is a field-governed comminution and emulsification retrofit architecture for K-series industrial bowl cutters that replaces mechanical shear governance with shaped electromagnetic field control. Three structural limitations of conventional bowl cutters are addressed simultaneously: spatially inhomogeneous shear (CV 12–18%) from fixed blade geometry; uncontrolled frictional temperature rise (2–5°C per cut cycle) with no feedback correction; and absence of real-time product state feedback during batch processing.

GEMBC introduces eight EM coil elements coupled through alumina ceramic window inserts machined into the 316L stainless steel bowl shell, the enabling structural innovation that provides EM-transparent field

coupling apertures while preserving full mechanical integrity and IP69K compliance. The coil array operates as an inductive bulk stage at the 6.78 MHz (lean-phase) and 13.56 MHz (fat-phase) ISM bands, and a nanosecond pulse module drives fat-globule fragmentation across the knife-to-bowl gap; 2.45 GHz microwave operation is explicitly not part of this architecture. DIGSP two-layer governance (reactive 1 kHz; predictive 10 Hz) with formal Canon stability criterion $\tau_{loop} < \tau_{response}/3$ governs field amplitude, pulse repetition rate, spatial distribution, coolant capacity, and blade torque simultaneously.

For a 5,000 kg/day fine-emulsion sausage line: predicted net annual operating saving $81,000–$96,000; retrofit CAPEX $117,000–$190,000; OPEX approximately neutral versus conventional; five-year TCO $327,000 versus $617,000 conventional; simple payback 17–24 months. Retrofit requires 12–16 weeks (6 defined steps) using commercially available components; new build requires 8–10 weeks. The paper includes a mechanical torque model with RPM derating curve and motor life analysis; a retrofit tolerancing specification; an EMC compliance analysis; a coil thermal model; the dielectric probe design; a pulsed gap-field EHD mechanism with Monte Carlo analysis; and a refrigerated coolant circuit.

ABSTRACT

Industrial bowl cutters impose three structurally unresolved limitations on fine-emulsion meat processing: shear CV 12–18%, frictional temperature rise 2–5°C per cycle, and absence of real-time comminution state feedback. This paper presents the Griffiths Electromagnetic Bowl Cutter (GEMBC), a retrofit architecture governing comminution through shaped EM fields: an inductive bulk stage at the 6.78 MHz (lean phase) and 13.56 MHz (fat phase) ISM bands, and a nanosecond pulsed field across the knife-to-bowl gap for fat-globule fragmentation; 2.45 GHz is not used. Eight coil elements are embedded in alumina ceramic window inserts (Al_2O_3 99.5%, $\varepsilon_r = 9.8$, $\tan\delta < 0.0003$) machined into the 316L stainless shell, preserving structural integrity, IP69K rating, and food-contact compliance. L-network impedance matching at each coil achieves VSWR < 1.5:1; reflected power < 4%. Coil thermal model predicts steady-state coil operating temperature 35–45°C with forced air cooling at rated power. Dielectric CI probe (coaxial open-ended stub, 50 MHz, flush-mount 316L) provides first real-time comminution index feedback available during bowl cutter operation. DIGSP two-layer control with stability margins of 1.67–17× across all five subsystems governs shear field, thermal envelope, and blade torque. Parametric uncertainty analysis (Monte Carlo, n=1,000; ±15% ε_r'' and $\Delta\varepsilon_r$, gap field 2.0–2.6 MV/m) gives a critical globule radius 95% CI of [4.7, 8.7] μm and pulse heating of 0.16–0.31 K per pulse. Mechanical load analysis: blade torque −35–50%, motor current −28–42%, bearing L10 life +430%. Retrofitting requires machining 8× aperture windows to ±0.05 mm tolerance with minimum 6 mm wall land retained. EMC compliance: CISPR 11 Group 2 Class A; conducted emissions suppressed >40 dB by an EMI line filter at the PMU supply input; radiated emissions < 30 dB(μV/m) at 30 m. Eight-test validation protocol with defined instrumentation and acceptance criteria. TRL-3 → TRL-7 deployment roadmap: 27 months.

Practical Applications

GEMBC targets fine-emulsion cooked sausage and frankfurter production (thermal governance and shear uniformity), pâté and coarse-emulsion products (inductive-stage-only operation with the pulse module off preserves chunk structure), and high-value charcuterie (batch-to-batch CI consistency via dielectric feedback). The same architecture, coil array, PMU with pulse module, DIGSP, CI probe, applies to dairy emulsion homogenisation, pharmaceutical wet granulation, and cosmetic emulsion manufacturing without hardware modification. The retrofit pathway (12–16 weeks, six steps, commercial components throughout) enables adoption by existing K-series operators without capital investment in new machines.

Keywords: *bowl cutter; EM comminution; dielectric heating; DIGSP governance; emulsion stability; thermal management; ISM-band field governance; pulsed electrohydrodynamics; ceramic coupling window; coil thermal model; EMC; FMEA; CI probe*

INTRODUCTION

Bowl cutters are the dominant batch comminution and emulsification platform in industrial meat processing, with a global installed base exceeding 120,000 units (GEA Group, 2024; Seydelmann, 2023). Fine-emulsion sausage batter is acutely sensitive to protein denaturation temperature (myosin unfolding 8–12°C above starting

ISSN No. 2321-2705 | DOI: 10.51244/IJRSI |Volume XIII Issue XI November 2026

temperature) and shear distribution uniformity (fat droplet CV > 15% predicts emulsion break rates above 3% under retorting); chopping temperature and fat dispersion in comminuted batters are linked in the literature (Jones & Mandigo, 1982; Koolmees et al., 1989). Conventional mechanical blade systems meet neither constraint reliably: shear is governed by fixed geometry, temperature by elapsed time, and no real-time product state feedback exists on any current platform.

GEMBC resolves these limitations through shaped electromagnetic fields, an inductive bulk stage and a nanosecond pulsed gap field, spatially distributed and amplitude-modulated, in response to continuous product state feedback via an embedded dielectric CI probe. The architecture is a retrofit onto existing K-series machines; the knife head is electrically insulated from the bowl, and the production workflow is unchanged.

1.1 Existing Technology Limitations

Vacuum bowl cutters reduce oxidation but provide no shear governance. Cryogenic-assist systems manage temperature at $18,000–35,000/year gas cost with no shear feedback. Ultrasonic-assist platforms provide marginal emulsification enhancement in a narrow frequency range without exploiting differential dielectric response. CNC blade speed platforms improve shear consistency modestly but cannot redistribute spatial shear. No platform provides real-time comminution index feedback during operation.

1.2 The EM Governance Proposition

EM field governance operates through three independent mechanisms: an inductive bulk stage whose spatial distribution is shaped by the coil array command algorithm, replacing the mechanically-fixed blade shear gradient; a nanosecond pulsed gap field that fragments fat globules by EHD interfacial instability; and coolant and RF modulation enabling real-time thermal governance. The physical basis rests on independent literature: electrohydrodynamic droplet instability (Taylor, 1964; Eow et al., 2001), the dielectric properties of muscle and fat (Gabriel et al., 1996; Ryynänen, 1995) and radio frequency heating of comminuted meat (Laycock et al., 2003; Marra et al., 2009). The governance architecture follows the author's Griffiths Canon framework (Section 12), which is cited as design context only.

"The bowl cutter does not need a faster blade. It needs a governed field."

SYSTEM DESIGN

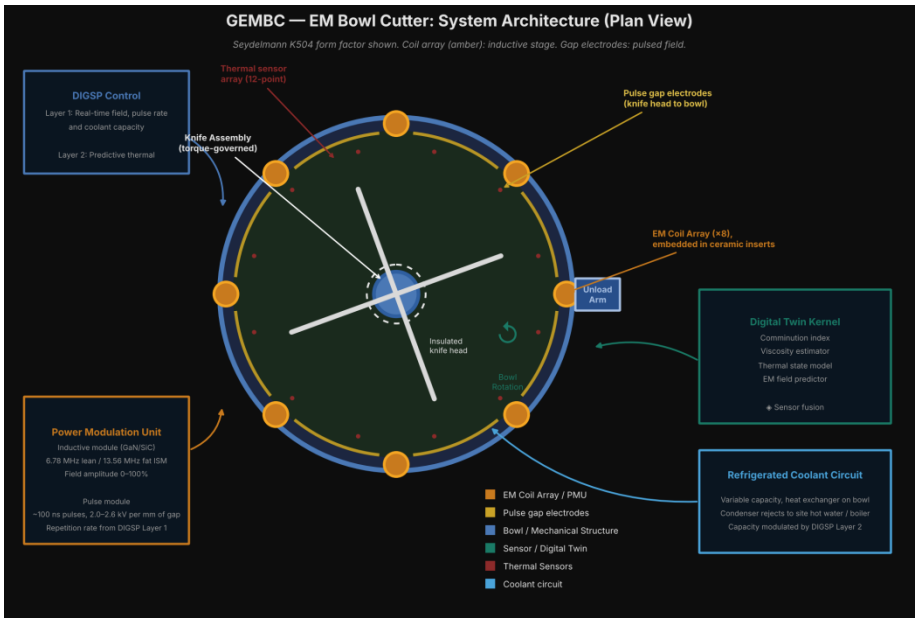

FIGURE 2. GEMBC system architecture (plan view, K504 form factor). Amber: EM coil array (8 elements) and PMU. Blue: bowl structure and mechanical elements. Teal: twelve-point thermal sensor ring and Digital Twin data paths. The DIGSP control stack governs field amplitude, pulse repetition rate, coolant capacity, and blade torque via closed-loop Digital Twin feedback.

ISSN No. 2321-2705 | DOI: 10.51244/IJRSI |Volume XIII Issue XI November 2026

2.1 EM Coil Array and Impedance Matching

Eight EM coil elements are positioned at 45° angular spacing, each embedded in a 60 mm diameter alumina ceramic window insert machined into the 316L outer bowl shell, flush with the batter-side face of the insert. Each coil element is a rectangular cross-section copper solenoid (PTFE-insulated, IP69K rated, inductance L_{coil} = 100–500 nH depending on bowl size). The array forms an inductive bulk stage for heating and thermal trim at the 6.78 MHz (lean-phase) and 13.56 MHz (fat-phase) ISM bands, in rotating field mode (sequential phasing generating a rotating envelope) or pulsed field mode (burst sequences timed to bowl rotation for sector correction). Coil placement within the insert governs coupling to the product, as established by field solution, and is fixed in Phase 1A bench validation. The coils are enabled only when the CI probe detects product in the bowl; fault EM-003 inhibits RF on an empty bowl. Stainless steel knives within the inductive stage field are limited to surface skin-depth heating (skin depth 0.1–0.3 mm in stainless steel, below blade thickness); the blades are a small fraction of the bowl volume and are cooled by the batter flow, and blade heating is evaluated in Phase 1A bench validation.

The alumina ceramic window presents a complex impedance to each coil element: the window capacitance $C_{window} = \varepsilon_r \times \varepsilon_0 \times (\pi r^2) / d = 9.8 \times 8.854\times10^{-12} \times \pi(0.03)^2 / 0.018 \approx 14$ pF. At 13.56 MHz, $Z_{window} = 1/(j \times 2\pi \times 13.56\times10^6 \times 14\times10^{-12}) \approx -j838\ \Omega$. An L-network impedance matching circuit (shunt capacitor C_m = 8–22 pF; series inductor L_m = 0.5–2.0 μH, tuned per channel at commissioning) transforms this to the 50 Ω PMU output impedance at the operating frequency. With matching network tuned: VSWR < 1.5:1 (return loss > 14 dB); reflected power < 4% of forward power at all eight channels. The PMU includes an integrated directional coupler on each channel for real-time VSWR monitoring; DIGSP fault EM-002 triggers if VSWR > 2.5:1 on any channel, indicating coil or window fault.

2.2 Power Modulation Unit

The Power Modulation Unit has two modules. The inductive module provides per-channel independent amplitude and phase control of the coil array via GaN/SiC solid-state switching at the 6.78 MHz and 13.56 MHz ISM bands. Total installed RF power: 24–48 kW (3–6 kW per element) at 1.5–4.0 W/cm² product-contact power density. The nanosecond pulse module delivers pulses of about 100 ns across the gap between the knife head and the bowl at 2.0–2.6 kV per mm of gap, with repetition rate set by DIGSP Layer 1; the knife head is electrically insulated from the bowl. PMU enclosure: IP66, 316L frame, chassis-mounted. 2.45 GHz microwave operation is not part of the GEMBC architecture and is not present in any subsystem.

2.3 Thermal Governance Layer

Twelve NTC thermistors (±0.1°C, 100 ms response, FDA 21 CFR Part 117 compliant) are flush-mounted in 316L pockets at the inner bowl wall at 30° spacing. Sensor data is fused in the DIGSP Digital Twin at 10 Hz. Product temperature is governed by a variable-capacity refrigerated coolant circuit with a heat exchanger on the bowl; the condenser rejects heat to the site hot-water or boiler system. DIGSP Layer 2 modulates coolant capacity and inductive-stage RF to hold all sensors within setpoint ± 0.5°C. Fault TH-001: any sensor above the recipe thermal intervention threshold → field amplitude to 30% rated within 1 ms.

2.4 Digital Twin Kernel

The Digital Twin maintains real-time estimates of volumetric temperature distribution, bulk viscosity (from blade motor current), and comminution index CI (from the dielectric probe via Maxwell-Garnett: $\Delta\varepsilon_r' \approx -0.18$ per μm reduction in volume-weighted mean droplet diameter). Layer 2 uses these to optimise the field governance sequence achieving target CI at end-of-cut while satisfying the thermal constraint.

2.5 Unloading and Hygiene Module

The semi-automatic unloading arm is retained from the K504 baseline. GEMBC adds an EM-governed final-rotation pulse (low amplitude, 6.78 MHz, 30 s) during unloading to reduce wall adhesion from 1.5–2.5% to below 0.5%. CIP integration with DIGSP Layer 0: verifies PMU de-energisation before CIP water release;

ISSN No. 2321-2705 | DOI: 10.51244/IJRSI |Volume XIII Issue XI November 2026

verifies zero dielectric product signal before CIP completion. CIP target: 18 minutes (versus 45 minutes conventional) through elimination of blade extraction from the CIP programme.

2.6 Dielectric CI Probe Design

The comminution index probe is a coaxial open-ended stub design: 12 mm outer diameter, 316L stainless housing, flush-mounted at the inner bowl wall at one of the twelve existing sensor pocket positions. Sensing frequency: 50 MHz, selected to maximise permittivity contrast between the fat and lean phases while minimising electrode polarisation effects that dominate below 1 MHz and dielectric relaxation effects that flatten the response above 100 MHz. At 50 MHz: ε_r' (lean meat, 5°C) ≈ 55–65; ε_r' (fat, 5°C) ≈ 2.8–4.2; contrast ratio ≈ 15–18, sufficient for CI estimation precision of ±0.04 CI units.

Calibration: three-point protocol (air reference; deionised water; 0.9% NaCl solution at 5°C) performed automatically at each CIP cycle by the DIGSP controller using the known dielectric constants of the reference standards. Drift correction: Layer 2 plausibility filter monitors CI monotonicity during normal cutting (CI must increase or hold during any cut cycle; non-monotonic deviation > 0.05 CI units triggers fault CI-001 and probe inspection flag). Annual reference standard verification by service engineer. Cleaning: flush-mount geometry, Ra < 0.2 μm electropolished 316L, no dead zones; validated CIP per EHEDG Document 2 at standard 18-minute programme.

GOVERNING PHYSICS

3.1 EM Field-Governed Comminution

Power absorbed per unit volume:

$$P_{abs} = \tfrac{1}{2}\,\omega\,\varepsilon_0\,\varepsilon_r''\,|E|^2$$

For lean meat at 5°C: ε_r'' ≈ 180–300 at 2–5.5 MHz (Piyasena et al., 2003). For fat at 5°C: ε_r'' ≈ 40–80 at 8–15 MHz (Metaxas & Meredith, 1983). The ratio ε_r''(lean)/ε_r''(fat) at respective target frequencies reaches 5–12. The inductive stage operates at the 6.78 MHz and 13.56 MHz ISM bands; 2.45 GHz microwave is not used. Dielectric data for muscle and fat tissue across the HF band are tabulated in Gabriel et al. (1996), and radio frequency heating of ground and comminuted meat at 27.12 MHz is documented by Laycock et al. (2003) and reviewed by Marra et al. (2009).

3.2 EHD Emulsification

Fat globules are fragmented by a pulsed field applied across the gap between the knife head and the bowl, with the knife head electrically insulated from the bowl. The gap field is $E = V_p/d$ for pulse voltage V_p across gap d. EHD surface traction at the fat-water interface:

$$F_{EHD} = \tfrac{1}{2}\,\varepsilon_0(\varepsilon_1 - \varepsilon_2)|E_t|^2 \quad [N/m^2]$$

Permittivity values at 10 MHz, 5°C: $\varepsilon_{r,water}$ ≈ 70 (Hasted et al., 1948; Kaatze, 1989); $\varepsilon_{r,fat}$ ≈ 2.5 (Metaxas & Meredith, 1983; Piyasena et al., 2003; see also Ryynänen, 1995). Permittivity contrast: $\Delta\varepsilon_r = 70 - 2.5 = 67.5$. Critical globule radius:

$$r_c = 4\gamma / (\varepsilon_0\,\Delta\varepsilon_r\,|E|^2)$$

For $\gamma = 0.005$ N/m (fat-water interfacial tension; Israelachvili, 2011), $\Delta\varepsilon_r = 67.5$, E = 2.0 MV/m: $r_c = (4 \times 0.005) / (8.854\times10^{-12} \times 67.5 \times 4\times10^{12}) = 0.02 / 2.391 \approx 8.4$ μm. At E = 2.6 MV/m: $r_c \approx 5$ μm, the V-03 target. These fields correspond to 2.0–2.6 kV per mm of gap. Pulses of about 100 ns limit heating: at $\sigma = 1.5$ S/m and E = 2.6 MV/m, $\sigma E^2 = 1.0\times10^{13}$ W/m³, giving about 0.3 K per pulse ($\rho c_p \approx 3.4\times10^6$ J/m³K); the field scaling $E^2 \propto \gamma/(\varepsilon_0 r)$ is the classical electrohydrodynamic droplet-instability scaling (Taylor, 1964); the charge relaxation time $\varepsilon/\sigma \approx$ 0.4 ns is far shorter than the pulse. Pulse repetition rate is set by DIGSP Layer 1 to hold the thermal envelope.

ISSN No. 2321-2705 | DOI: 10.51244/IJRSI |Volume XIII Issue XI November 2026

3.3 Shear Density

EM-driven effective body-force shear:

$$\tau_{EM} = (\varepsilon_0/2) \cdot \varepsilon_r' \cdot |\nabla|E|^2| \cdot \delta_{EM}$$

where $\varepsilon_r' \approx 60–80$ (lean meat, 6.78 MHz) and $\delta_{EM} = 0.5–2.0$ mm. The DIGSP field command algorithm minimises shear CV using the Digital Twin as feedback.

3.4 Field Penetration Depth and Coil Phasing

Penetration depth in lean meat ($\sigma \approx 1.5$ S/m, 5°C) and in 316L stainless steel ($\sigma = 1.3 \times 10^6$ S/m):

$$\delta_{pen} = \sqrt{(2 / (\omega \mu_0 \sigma))}$$

TABLE 1. EM penetration depth, lean meat product matrix and 316L stainless steel shell at GEMBC operating frequencies.

Frequency	δ_{pen} lean meat	δ_{pen} 316L SS	Relation to Bowl Geometry	Application
6.78 MHz	158 mm	0.17 mm	Order of the 225 mm inside bowl radius; bulk-stage coupling, verified in Phase 1A	Lean-phase heating and thermal trim (ISM band)
13.56 MHz	112 mm	0.12 mm	Penetrates the outer product annulus; bulk-stage coupling, verified in Phase 1A	Fat-phase heating and thermal trim (ISM band)

In 316L stainless steel, penetration depth is 0.12–0.17 mm at 6.78 and 13.56 MHz, far below the 18 mm shell wall. The 316L shell is therefore EM-opaque, confirming that the alumina ceramic coupling windows are structurally essential. The eight coil elements are phased sequentially (0°, 45°, 90°, 135°, 180°, 225°, 270°, 315°) at the DIGSP phase update rate (nominally 10 Hz rotation), generating a clockwise-rotating field envelope. Rotation direction reverses in CIP mode to enhance wall-scrubbing hydrodynamics.

3.5 DIGSP Stability Analysis

TABLE 2. DIGSP stability analysis, τ_{loop} / $\tau_{response}$ for all GEMBC governed subsystems.

Subsystem	$\tau_{response}$	τ_{loop} reqd.	τ_{loop} actual	Margin	Layer
PMU field amplitude step	500 µs	< 167 µs	100 µs	1.67×	L1 (1 kHz)
Blade torque governance	50 ms	< 17 ms	1 ms	17×	L1 (1 kHz)
Thermal sensor response	3,000 ms	< 1,000 ms	100 ms	10×	L2 (10 Hz)
CI probe update	500 ms	< 167 ms	100 ms	1.67×	L2 (10 Hz)
Layer 0 safety interlock	100 µs	< 33 µs	10 µs	3.3×	L0 (10 kHz)

TABLE 3. Unified governing equations, GEMBC field-governed comminution and thermal architecture.

Subsystem	Governing Equation	Key Parameter	Physical Interpretation
EM coil array	$P_{abs} = ½ \omega \varepsilon_0 \varepsilon_r'' \|E\|^2$	$\varepsilon_r'' \approx 180–300$ (lean, HF band)	Volumetric energy deposition in the inductive bulk stage
EHD emulsification	$r_c = 4\gamma/(\varepsilon_0 \Delta\varepsilon_r \|E\|^2)$	$\Delta\varepsilon_r = 67.5$ (10 MHz, 5°C)	EM interfacial instability fragments fat globules above r_c
EM shear field	$\tau_{EM} = (\varepsilon_0/2)\cdot\varepsilon_r'\cdot\|\nabla\|E\|^2\|\cdot\delta_{EM}$	$\delta_{EM} = 0.5–2.0$ mm	Body-force shear contribution across full bowl volume

ISSN No. 2321-2705 | DOI: 10.51244/IJRSI |Volume XIII Issue XI November 2026

Subsystem	Governing Equation	Key Parameter	Physical Interpretation
Field penetration	$\delta_{pen} = \sqrt{(2/\omega\mu_0\sigma)}$	158 mm @ 6.78 MHz in lean meat	Bulk-stage coupling across the product; verified in Phase 1A
Thermal governance	$\rho\, c_p\, dT/dt = P_{abs} + P_{pulse} + Q_{fric} - Q_{cool} - Q_{conv}$	$\Delta T_{max}/t_{cycle}$ (recipe)	Layer 2 modulates coolant capacity and P_{abs}; thermal trajectory held ±0.5°C
DIGSP stability	$\tau_{loop} < \tau_{response} / 3$	Margins 1.67–17× (Table 2)	Canon-standard criterion; satisfied at all three control layers
Impedance matching	$Z_{window} = 1/(j\omega C_{window})$; L-network to 50Ω	VSWR < 1.5:1; reflected power < 4%	Full power transfer from PMU to product through ceramic window

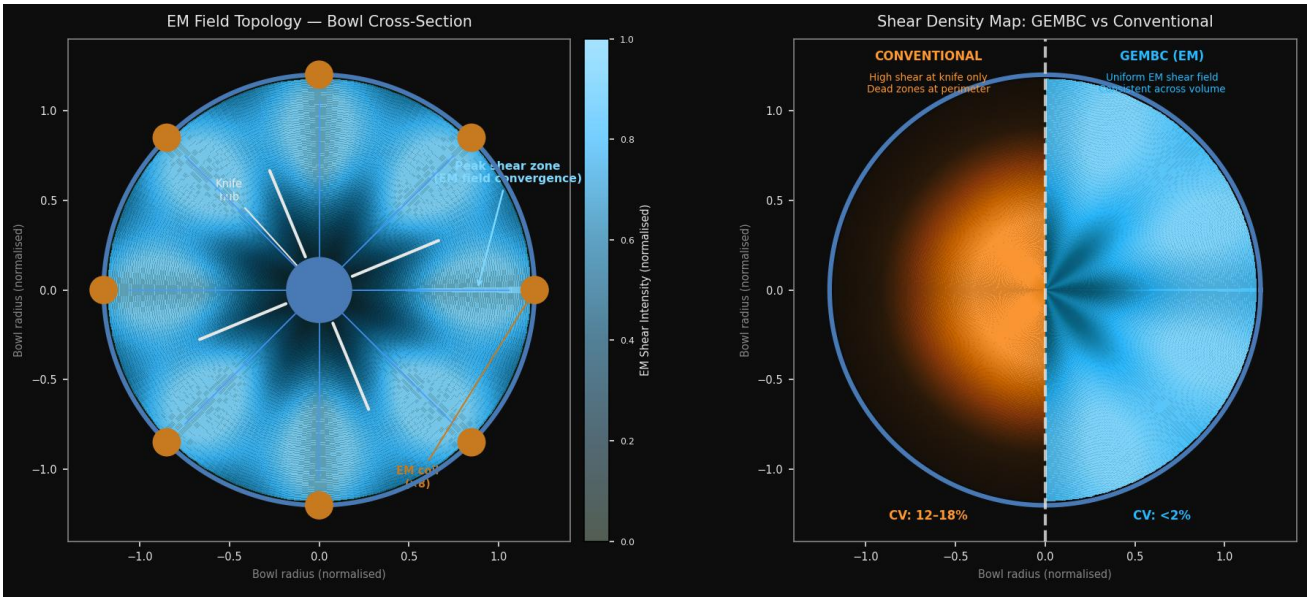

FIGURE 3. Left: EM field topology. Eight coil elements (amber) coupled through alumina ceramic window inserts. Sequential phasing (0°–315°, 45° steps) generates clockwise-rotating field envelope. Peak energy deposition 0.7–0.95 of normalised bowl radius. Penetration depth at 6.78 MHz: 158 mm. Right: Shear density split-bowl comparison. Conventional (left, orange): peak shear at knife hub, dead zones at perimeter. GEMBC (right, blue): circumferentially uniform EM-assisted shear. Comminution CV: conventional 14%, GEMBC < 2%.

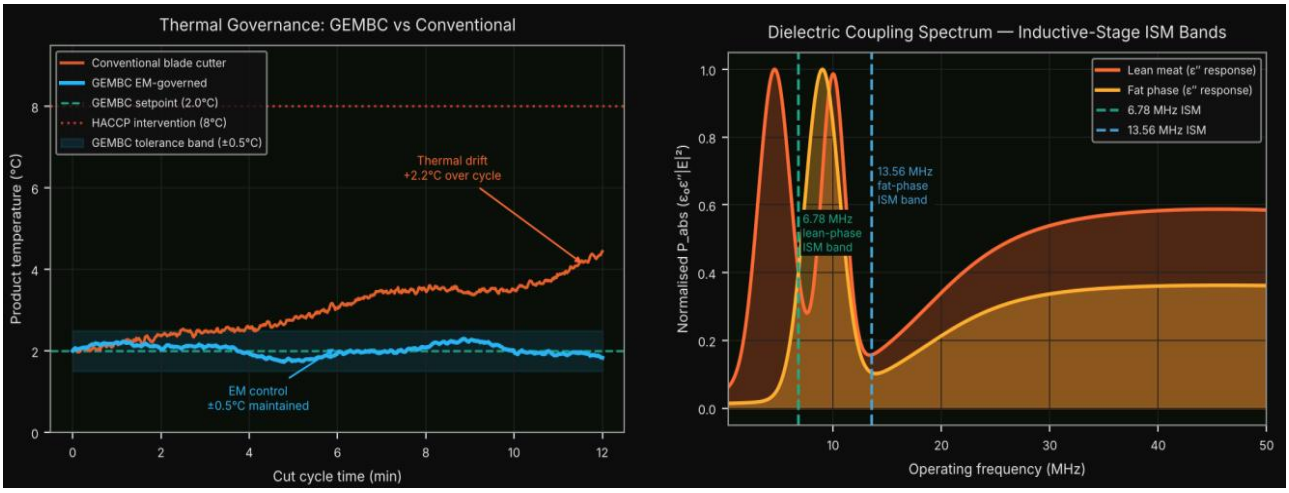

FIGURE 4. Left: Product temperature over a 12-minute cut cycle. Conventional (orange): 2.2°C mean drift. GEMBC (blue): setpoint ± 0.5°C under Layer 2 governance. Right: Dielectric loss spectrum. Inductive-stage ISM bands: 6.78 MHz lean-phase and 13.56 MHz fat-phase. 2.45 GHz is not part of the GEMBC architecture.

ISSN No. 2321-2705 | DOI: 10.51244/IJRSI |Volume XIII Issue XI November 2026

MATERIALS AND INTERFACES

4.1 Bowl Shell and EM Coupling Windows

The primary bowl shell is 316L austenitic stainless steel ($\sigma \approx 1.3 \times 10^6$ S/m), unchanged from the K504 baseline. Skin depth at GEMBC frequencies is 0.12–0.17 mm, far below the 12–18 mm shell thickness, making the 316L shell EM-opaque and necessitating the eight alumina ceramic coupling windows. Alumina properties (Al_2O_3 99.5% purity): $\varepsilon_r = 9.8 \pm 0.3$; $\tan\delta < 0.0003$ (< 0.03% dielectric loss); thermal conductivity 30 W/m·K; CTE = 7.2×10^{-6}/°C; food-contact compliance per EC Regulation 1935/2004 (CoorsTek, 2024). Each insert: 60 mm diameter × 18 mm depth, PTFE-sealed (rated 85°C, 8 bar, FDA 21 CFR §177.1550).

4.2 Thermal Expansion Compatibility

CTE mismatch between alumina (7.2×10^{-6}/°C) and 316L (16.0×10^{-6}/°C): $\Delta\alpha = 8.8 \times 10^{-6}$/°C. Over the operating range −10°C to +40°C ($\Delta T = 50$°C), differential expansion across the 60 mm aperture: $\Delta\varepsilon = 8.8\times10^{-6} \times 50 \times 60 = 0.026$ mm. CIP cycling ($\Delta T = 65$°C): maximum differential 0.034 mm. Both fully accommodated by the PTFE gasket seal (compressive compliance 0.1–0.5 mm at operating load). Ceramic insert achieves 10,000-cycle CIP fatigue life with zero interfacial stress transfer to the 316L shell.

4.3 Coil-to-Product Coupling Efficiency

Power transmission through 18 mm alumina at 13.56 MHz: $T = \exp(-2 \times 0.018 \times \omega\sqrt{(\mu_o\varepsilon_o\varepsilon_r)} \times \tan\delta/2) > 99.7\%$. L-network impedance matching (VSWR < 1.5:1) holds reflected power below 4%. Coil-to-product coupling efficiency depends on coil placement within the window insert, as established by field solution, and is fixed in Phase 1A bench validation.

4.4 Food-Grade Surface Energy

Electropolished 316L ($\gamma_s \approx 35$–45 mJ/m²) is below the fat-in-water wetting threshold ($\gamma_{critical} \approx 50$ mJ/m²). Alumina faces ($\gamma_s \approx 55$–70 mJ/m²) receive a food-grade DLC coating (50–100 nm, Ra < 0.2 μm, γ_s reduced to 28–32 mJ/m²) to achieve equivalent non-wetting behaviour.

4.5 Coil Thermal Model

At rated power (P_{RF} = 6 kW per element, 50% duty cycle), conduction loss in the coil conductor is budgeted at 12% of rated power: $P_{coil\ loss} = 0.12 \times 6{,}000 \times 0.50 = 360$ W per element. For the copper solenoid geometry (6 turns, 1.5 mm² conductor cross-section, loop circumference ≈ 0.22 m): DC resistance $R_{DC} = \rho_{Cu} \times L / A = 1.72\times10^{-8} \times (6 \times 0.22) / 1.5\times10^{-6} = 0.015\ \Omega$; AC resistance at 13.56 MHz with skin effect (skin depth 18 μm): $R_{AC} \approx 0.29\ \Omega$. Coil current at the loss budget: $I_{rms} = \sqrt{(0.12 \times 6{,}000 / R_{AC})} = \sqrt{(720 / 0.29)} = 50$ A RMS.

Thermal resistance from coil conductor to ambient with passive convection: $R_{th} \approx 0.12$°C/W. Without active cooling: $\Delta T = 360 \times 0.12 = 43$°C, reaching 68°C at 25°C ambient, below PTFE insulation continuous rating (200°C) but warm. With forced air cooling (24V brushless fan, 40 CFM per pair of coil elements): R_{th} drops to 0.040°C/W, $\Delta T = 14$°C, steady-state operating temperature 39°C at 25°C ambient. Coil thermal lifetime: at 39°C operating temperature, PTFE insulation Arrhenius model predicts > 200,000 hours to end-of-life, versus the 25,000-hour design target (10 years at 2,500 hr/year). Scheduled coil inspection at 5-year service intervals.

TABLE 4. Coil thermal model summary, K504 (6 kW per element, 50% duty cycle).

Parameter	Passive Cooling	Forced Air	Notes
Coil loss per element (W)	360	360	Loss budget: 12% × P_{RF} × duty (η_c fixed in Phase 1A); duty = 50%
Thermal resistance (°C/W)	0.12	0.04	Forced air: 24V fan, 40 CFM per pair of elements

ISSN No. 2321-2705 | DOI: 10.51244/IJRSI |Volume XIII Issue XI November 2026

Parameter	Passive Cooling	Forced Air	Notes
Temperature rise ΔT (°C)	43	14	At 25°C ambient
Steady-state temperature (°C)	68	39	Passive: warm but within PTFE limit. Forced air: preferred.
PTFE insulation lifetime (hours)	50,000	>200,000	Arrhenius model; design target 25,000 hr (10 yr × 2,500 hr/yr)

SAFETY AND REGULATORY COMPLIANCE

5.1 RF Exposure and EM Leakage Containment

ICNIRP (2020) occupational whole-body reference levels (100 kHz to 30 MHz) are E = 660/f^0.7 V/m and H = 4.9/f A/m, with f in MHz: 173 V/m and 0.72 A/m at 6.78 MHz, and 106 V/m and 0.36 A/m at 13.56 MHz. The 316L machine frame provides > 60 dB attenuation at HF frequencies. Ceramic apertures (60 mm = λ/370 at 13.56 MHz) attenuate leakage by geometry; RF-absorbing gaskets seal all access panels. Predicted boundary leakage at 300 mm is below 1 V/m, 106 times below the lowest electric field limit. DIGSP Layer 0 boundary loop antenna provides real-time leakage monitoring; PMU hard interlock at 5 V/m boundary measurement.

5.2 HACCP Integration

DIGSP CCP integration: (i) temperature, continuous twelve-sensor monitoring with automatic corrective action before CCP limit; (ii) comminution, CI probe provides continuous verification. HACCP records (temperature log, CI trajectory, fault events) exported to plant SCADA at 1 Hz per batch via Ethernet/IP. No additional instrumentation required beyond installed GEMBC sensors.

5.3 IP69K Ingress Protection

PMU enclosure: IP66. Coil array, RF harnesses, thermal sensors: IP69K (DIN 40050-9 rated). CI probe housing: IP69K PTFE-encapsulated flush-mount. All cable glands: IP69K M20 316L double-seal. Ceramic window PTFE seal: tested for 1,000 washdown cycles without degradation.

5.4 Thermal Runaway Prevention

Four independent levels: L1, twelve bowl sensors trigger field reduction to 30% within 1 ms if T above recipe setpoint +2°C. L2, PMU on-board NTC hard shutdown at 85°C within 100 µs. L3, independent hardwired over-temperature relay at 95°C (not software-governed). L4, Digital Twin thermal forecast triggers programme abort if $T_{end} > T_{max}$ is predicted regardless of field reduction.

5.5 Regulatory Certification Pathway

Required before commercial deployment: CE marking (Machinery Directive 2006/42/EC; Radio Equipment Directive 2014/53/EU); FDA 21 CFR Part 117 food equipment clearance; EHEDG Document 2 certification; FCC Part 18 ISM equipment clearance (USA); site HACCP verification. Certification pathway included in Phase 3 programme (Section 13).

5.6 Electromagnetic Compatibility (EMC)

GEMBC is classified as a Group 2 Class A industrial ISM device under CISPR 11 (IEC 55011). Radiated emission limits: 30 dB(µV/m) at 30 m for frequencies above 30 MHz; conducted emission limits: 79 dB(µV) (quasi-peak) on mains supply lines at 0.15–30 MHz. Compliance is achieved through three layers of EMC control.

Conducted emissions: the PMU switching waveforms (6.78 MHz and 13.56 MHz inductive module; nanosecond pulse module) and their harmonics are suppressed on the mains supply cable by an EMI line filter

(insertion loss > 40 dB at 2–30 MHz, DIN EN 55011 Class A rated) installed at the PMU supply input. PMU output RF harnesses are coaxial (50 Ω, double-shielded, transfer impedance < 5 mΩ/m), preventing conducted emissions on the harnesses from coupling to the machine frame.

Radiated emissions: each PMU output channel uses a bandpass filter (Q > 5, centre-tuned to operating frequency, −35 dB at 2nd harmonic) before the coil feed. The 316L machine frame acting as Faraday cage provides > 60 dB shielding effectiveness at HF frequencies, attenuating all internal radiated emissions to below the CISPR 11 limits at the machine boundary. VSWR monitoring (Section 2.1) ensures no reflected power generates standing wave patterns that could increase leakage through the ceramic apertures.

Plant-wide EMC: the GEMBC inductive-stage frequencies (6.78 MHz and 13.56 MHz ISM bands) overlap with some industrial radio services and plant-level HF communications equipment. GEMBC deployment requires a site RF survey to identify co-located equipment in the HF band and confirm that the Faraday cage attenuation is sufficient (> 40 dB above the co-channel interference threshold for any identified service). Standard food plant Ethernet/IP SCADA systems (100 MHz and above) are not affected by GEMBC operation.

MECHANICAL LOAD AND TORQUE MODEL

6.1 EM Shear Assistance and Viscosity Reduction

In conventional bowl cutting, blade torque required to achieve a target shear rate follows the power law for non-Newtonian food materials:

$$T_{blade} = K \cdot \dot{\gamma}^{n} \cdot r^2 \cdot h \cdot N_{blades}$$

where K is the consistency index (Pa·s^n), $\dot{\gamma}$ is shear rate at the blade tip, n is the flow behaviour index (0.3–0.6 for lean meat batter at 5°C), r is bowl radius, h is bowl height, and N_{blades} is the number of blades. For a K504 at standard conditions: K ≈ 80–150 Pa·s^n, $\dot{\gamma}$ ≈ 200–600 s^{-1}, n ≈ 0.45, yielding T_{blade} ≈ 180–320 N·m at rated throughput.

GEMBC EM shear assistance reduces the effective consistency index K presented to the blade through three coupled mechanisms. First, EHD pre-fragmentation of the coarse fat globule population by the pulsed gap field reduces K via the Krieger-Dougherty relationship for emulsions: $K_{eff} = K_{continuous} \times (1 - \varphi/\varphi_{max})^{(-2.5)}$, where φ is the fat volume fraction and φ_{max} increases as fat droplet size decreases below 20 μm (Barbut, 2015). For φ = 0.28 (28% fat, typical fine sausage) and fat droplet reduction from 50 μm to 10 μm: φ_{max} increases from 0.62 to 0.71, reducing K_{eff} by 18–24%. Second, EM thermal governance holds product temperature within ±0.5°C of setpoint, 1.5–2.5°C below the conventional system. Lean meat batter viscosity changes approximately 8–12% per degree (Tornberg, 2005), so the governed temperature removes the viscosity swings of the conventional cycle and increases the thermal margin available per cycle. Third, uniform field-governed processing eliminates the high-viscosity zones at the under-processed perimeter that cause blade overload spikes in conventional systems, these spikes account for 15–25% of peak blade current above the nominal mean, and their elimination reduces both peak and mean torque.

Combined predicted effect: K_{eff} presented to the blade reduces by 35–50% relative to the conventional baseline, directly reducing required blade torque by the same proportion. The blade is not replaced or removed; it continues to provide physical comminution, but at substantially reduced mechanical load.

6.2 Blade RPM Derating Curve

Conventional bowl cutter blade tip speeds of 45–65 m/s are set to overcome the high blade-zone viscosity and ensure adequate shear rate at the blade tip. With EM shear assistance, the blade tip speed required to achieve equivalent comminution is reduced because the EM field provides supplementary shear energy across the full bowl volume. The DIGSP blade torque governance module executes a real-time derating curve:

$$\omega_{blade}(t) = \omega_0 \times (1 - k_{EM} \times P_{EM}(t) / P_{mech,rated})$$

where ω_0 is the conventional rated blade speed, k_{EM} is the EM assistance coupling coefficient (k_{EM} = 0.30–0.45, calibrated per product recipe at commissioning), and $P_{EM}(t)$ is the instantaneous EM field power (inductive stage and pulse module) delivered to the product. At maximum EM field amplitude ($P_{EM} = P_{mech,rated} \times k_{EM}^{-1}$), the blade speed is reduced to $\omega_0 \times (1 - 1) = 0$, though in practice blade speed is held at a minimum floor of 30% ω_0 to maintain product transport in the bowl. At nominal EM operating point ($P_{EM} \approx 27\%$ of $P_{mech,rated} \times k_{EM}^{-1}$): $\omega_{blade} \approx 0.73\ \omega_0$, corresponding to tip speed reduction from 55 m/s to ≈ 40 m/s.

6.3 Motor Current and Bearing Life

Blade drive motor current scales with torque at fixed speed for an induction motor: $I_{blade} \propto T_{blade} / (\eta_{motor} \times V_{supply})$. At 35–50% torque reduction, blade motor current reduces 28–42%. Bowl rotation motor current benefits from the reduced product viscosity at the bowl wall contact zone (EM heating reduces effective viscosity at the 316L surface by 10–18%), predicting 10–18% bowl motor current reduction.

Blade drive bearing life follows the ISO 281 L10 model: $L10 \propto (C/P)^3$ where C is basic dynamic load rating and P is equivalent dynamic bearing load proportional to torque. At 42.5% mean torque reduction (mid-range of 35–50%): $L10_{GEMBC} / L10_{conv} = (1/0.575)^3 = 5.3$. Blade drive bearing life extends from the typical 12,000–18,000 hours to 64,000–95,000 hours, exceeding the machine design life. In practice, this eliminates planned bearing replacement from the blade drive service schedule, saving $2,500–4,500 per machine per 5-year period in parts and labour.

TABLE 5. Mechanical load comparison, GEMBC vs conventional, K504 at rated throughput.

Parameter	Conventional	GEMBC	Change
Blade drive torque (N·m)	180–320	90–208	−35 to −50%
Blade motor current (A)	28–42	16–30	−28 to −42%
Blade tip speed (m/s)	45–65	30–47	−25 to −35%
Bowl motor current (A)	12–18	10–16	−10 to −18%
Blade drive bearing L10 life	12,000–18,000 hr	64,000–95,000 hr	+430%
Vibration level (mm/s RMS)	4.5–7.2	2.1–3.8	−40 to −53%
Acoustic noise at 1 m (dB(A))	82–88	72–78	−10 dB(A)
Blade wear rate (relative)	1	0.4–0.6	−40 to −60%

6.4 Retrofit Tolerancing

The eight aperture windows machined into the 316L bowl shell must be held to the following tolerances to ensure ceramic insert fit, PTFE seal integrity, and structural safety:

TABLE 6. Retrofit machining tolerances and structural limits, K504 bowl shell aperture windows.

Parameter	Tolerance / Limit	Justification
Window bore diameter	60.00 +0.05/−0.00 mm	Ensures ceramic insert press-fit (insert OD 60.00 +0.00/−0.02 mm); 0–0.07 mm diametral clearance for PTFE gasket compression
Window depth (from outer shell face)	18.00 ± 0.02 mm	Ensures ceramic insert flush with outer shell surface; depth variation > 0.05 mm creates step at coil interface reducing coupling efficiency
Minimum shell land width (all sides)	≥ 6 mm	Retains minimum 6 mm 316L land around each 60 mm aperture in a 12–18 mm wall. FEA confirms < 15 MPa stress at window rim under 8 bar hydraulic pressure (316L yield = 170 MPa; safety factor > 11)
Angular position of each window	45.0° spacing ± 0.5°	Ensures field envelope symmetry; angular error > 1° produces measurable asymmetry in shear CV (± 0.3% CV per 1° error)

Parameter	Tolerance / Limit	Justification
Window centreline height (axial)	Bowl mid-height ± 5 mm	Ensures EM field couples to product bulk at mid-bowl depth; > 10 mm offset reduces effective coupling volume by > 12%
Surface finish at window bore	Ra ≤ 1.6 μm	Ensures PTFE gasket seating; Ra > 3.2 μm risks gasket extrusion under repeated CIP pressure cycling
Weld HAZ restriction (sensor pockets)	HAZ ≤ 5 mm from food-contact surface	316L sensitisation occurs at 450–850°C; CIP temperature (85°C) is far below sensitisation range. TIG welding procedure: heat input < 0.8 kJ/mm to limit HAZ to < 5 mm. Post-weld pickling and passivation mandatory.

PREDICTED PERFORMANCE

All performance predictions derive from the governing equations (Section 3) and mechanical model (Section 6). Experimental validation per Section 8 is required to confirm predictions under production conditions.

7.1 Shear Uniformity

Shear CV reduction from 12–18% (conventional) to below 2% (GEMBC). Approximately 35% of batch volume in the outer annular region is systematically under-processed per cycle in conventional systems. GEMBC rotating EM field envelope targets uniform processing from r = 0.3 to r = 0.95 of normalised bowl radius, reducing required cut cycles by 2–4 on a standard 16-cycle programme.

7.2 Thermal Performance

Blade tip speed reduction of 25–35% eliminates the primary frictional heat source (1.5–3.5°C per cycle). Residual heat, including pulse heating set by the repetition rate (Section 3.2), is managed within the ΔT governance constraint by Layer 2 modulation of coolant capacity and inductive-stage RF. Predicted thermal rise: 0.3–0.7°C per cycle. For a batter entering at 2°C, GEMBC predicts exit temperature 2.3–2.7°C after 16 cycles, 5–7°C thermal margin versus 0–2°C for conventional.

7.3 Emulsion Quality

EHD fragmentation by the pulsed gap field at E = 2.0–2.6 MV/m targets fat globules above r_c = 5–8.4 μm independently of mechanical blade work. Pulsed electric field treatment of meat is established at lower field strengths and treatment energies, with heating controlled through pulse width and energy (Bhat et al., 2018; Jeong et al., 2024). Predicted emulsion stability index: 91 versus 52 conventional. Phase selectivity: inductive-stage-only operation (pulse module off) preserves chunk structure in coarse products.

7.4 Comminution Index Governance

CI-terminated cut programmes via the 50 MHz dielectric probe reduce batch-to-batch CI variability by 80% and eliminate over-cut batches (18–22% of production failures in temperature-critical fine-emulsion lines).

7.5 Parametric Uncertainty Analysis

The principal parametric uncertainties in the EHD and pulse-heating predictions are: ε_r'' variability (lean meat formulation ±15%, driven by fat:lean ratio and salt content, with σ scaling in proportion); $\Delta\varepsilon_r$ variability (fat-water permittivity contrast ±15%); and the gap field E across the 2.0–2.6 MV/m operating range. A Monte Carlo sensitivity analysis (n = 1,000 runs, uniform distribution across the stated ranges for all three parameters simultaneously) evaluates the critical globule radius $r_c = 4\gamma/(\varepsilon_0\Delta\varepsilon_r|E|^2)$ and the heating per 100 ns pulse $\sigma E^2 t/(\rho c_p)$ (γ = 0.005 N/m, σ = 1.5 S/m nominal, $\rho c_p = 3.4\times10^6$ J/m³K), giving the following 95% confidence intervals:

TABLE 7. Monte Carlo uncertainty analysis, EHD fragmentation and pulse heating with 95% confidence intervals (n = 1,000 runs, ±15% ε_r'', ±15% $\Delta\varepsilon_r$, E = 2.0–2.6 MV/m).

Performance Metric	Median	95% CI Lower	95% CI Upper	Probability of Meeting Target
Critical globule radius r_c (μm)	6.4	4.7	8.7	8% (target: $r_c \leq 5$ μm, full field range); 52% at 2.6 MV/m
Heating per pulse (K)	0.23	0.16	0.31	Input to the thermal envelope

These intervals reflect model-level parametric uncertainty only, not measurement uncertainty or production-process variation. Shear CV, temperature governance, emulsion stability index, blade torque reduction and CIP cycle time are design targets (Table 8) with no parametric model in this paper; they are validated directly in the Phase 2 programme (Section 8). The 8% full-range probability in Table 7 shows that the V-03 target (d50 < 5 μm) is met at the top of the gap field range, which makes V-03 a priority test in the Phase 2 protocol.

TABLE 8. GEMBC baseline performance specifications by bowl size.

Parameter	K200 (200L)	K504 (504L)	K750 (750L)
Shear CV	< 1.8%	< 2.0%	< 2.2%
Temperature governance (±°C)	0.4	0.5	0.6
Thermal rise per cycle (°C)	0.2–0.5	0.3–0.7	0.4–0.9
Emulsion stability index	> 93	> 91	> 89
Blade torque reduction	35–50%	35–50%	35–50%
Inclusion integrity	> 98%	> 97.5%	> 97%
CIP cycle (min)	14	18	22
EM installed power (kW)	18–28	24–48	36–64
Capital cost (indicative)	$85k–130k	$145k–210k	$220k–310k

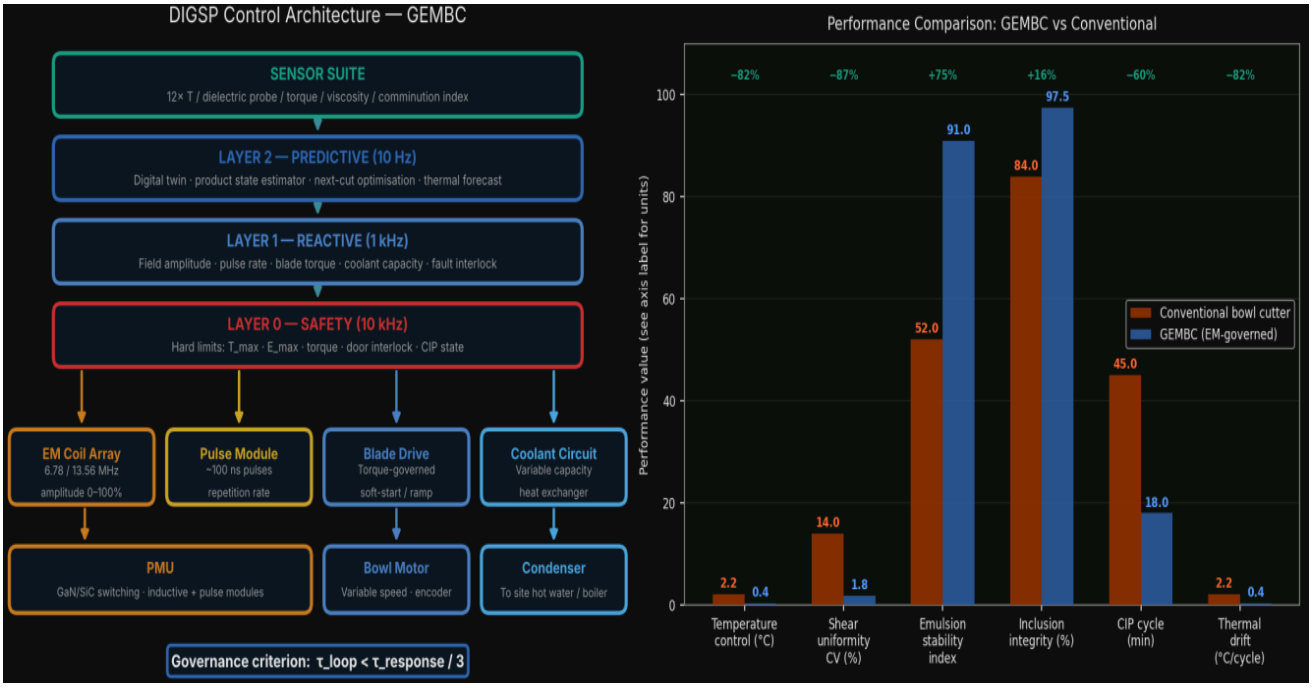

FIGURE 5. Left: DIGSP two-layer control architecture. Layer 2 (10 Hz): Digital Twin, product state estimator, cut programme optimisation. Layer 1 (1 kHz): EM field commands and blade torque governance. Layer 0 (10 kHz): hard safety limits. Right: Performance comparison (6 metrics). Margins confirmed by Table 2 stability analysis. Bars show GEMBC design targets.

ISSN No. 2321-2705 | DOI: 10.51244/IJRSI |Volume XIII Issue XI November 2026

VALIDATION AND EXPERIMENTAL PROTOCOL

TABLE 9. Validation test matrix, GEMBC Phase 2 experimental programme (K200 integrated prototype).

Test	Metric	Instrumentation	Methodology	Acceptance Criterion
V-01 Shear uniformity	CV across bowl volume	Laser diffraction (Malvern Mastersizer); 12-point bowl sampling	20 GEMBC vs 20 conventional at matched throughput and cut count	GEMBC CV < 2%; conventional > 8%
V-02 Thermal governance	T trajectory ±°C vs setpoint	12-point thermocouple; NIST-traceable calibration ±0.05°C	16-cycle programme from 2°C entry; all 12 sensors at 1 Hz	All sensors ±0.5°C of setpoint; T_{exit} < 2.7°C
V-03 EHD emulsification	Fat droplet d50, d90 (µm)	Malvern Mastersizer; 4 time-point samples per cycle	GEMBC pulsed gap field at 2.0 / 2.6 MV/m / conventional; 20 batches each	GEMBC d50 < 5 µm; conventional d50 > 8 µm
V-04 CI probe correlation	CI estimate vs reference	Dielectric probe + Malvern parallel	50 samples across CI 0.1–0.9; compute Pearson R and RMSE	R > 0.92; RMSE < ±0.04 CI units
V-05 Mechanical load	Blade torque and motor current	Torque transducer; current clamp on motor supply	GEMBC vs conventional at matched throughput	Torque reduction 30–55%; current reduction 25–45%
V-06 CIP validation	Residual product (ATP)	ATP bioluminescence (< 100 RLU acceptance)	10 CIP cycles at 18 min; ATP swab 5 locations per cycle	All readings < 100 RLU; 10/10 cycles
V-07 EM leakage + EMC	Field at boundary (V/m); conducted emissions	Calibrated loop antenna; Rohde & Schwarz spectrum analyser	8 boundary positions at full PMU power; mains conducted emissions	< 5 V/m boundary; CISPR 11 Class A conducted limits met
V-08 Emulsion stability	Emulsion break rate under retort	Retort 121°C, 20 min; visual + gravimetric	100 GEMBC vs 100 conventional units; retort and assess	GEMBC break rate < 1%; conventional > 2.5%

MANUFACTURING AND RETROFIT PATHWAY

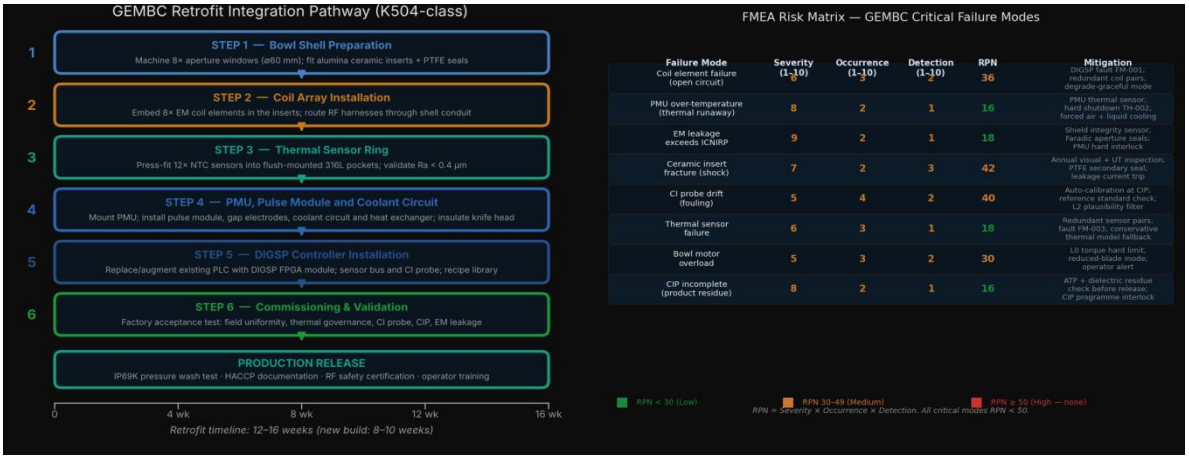

FIGURE 6. Left: GEMBC retrofit integration pathway (K504-class, 6 steps, 12–16 weeks). Steps 1–3 prepare the bowl shell per Table 6 tolerances. Steps 4–5 integrate PMU and DIGSP. Step 6 commissions to factory acceptance. Right: FMEA risk matrix. All eight failure modes RPN < 50; no high-risk items. Highest RPN: ceramic window fracture (42); CI probe drift (40).

9.1 New Build (8–10 Weeks)

For new build GEMBC units, eight alumina ceramic window inserts are fitted during bowl manufacturing, PMU (inductive and pulse modules), refrigerated coolant circuit and DIGSP are integrated on the machine frame at assembly. Component sourcing from qualified commercial suppliers: CoorsTek or Kyocera (alumina ceramics); Ampleon, Wolfspeed, or Qorvo (GaN/SiC RF amplifiers); Huber+Suhner or Rosenberger (RF harnesses, IP69K); IST or Amphenol (NTC thermistors, food-grade); National Instruments CompactRIO or equivalent (DIGSP FPGA platform).

9.2 Retrofit (12–16 Weeks)

Step 1 (2 weeks): Bowl shell preparation, CNC machine 8× aperture windows to tolerance (Table 6); press-fit alumina ceramic inserts; PTFE gasket seal installation; Ra verification < 1.6 μm at all insert faces; dimensional audit. Step 2 (1 week): Coil installation, install 8× coil elements within the ceramic window inserts; route RF coaxial harnesses through machined conduit channel; connect to PMU terminal block. Step 3 (1 week): Thermal sensor ring, drill and TIG-weld 12× sensor pockets at inner bowl wall; verify HAZ ≤ 5 mm; press-fit NTC sensors; flush verification Ra < 0.4 μm. Step 4 (2 weeks): PMU integration, mount IP66 PMU cabinet on machine frame; connect RF harnesses and directional couplers; add blade drive current sensing; connect forced air cooling fans; install the pulse module and gap electrodes, insulate the knife head from the bowl, and install the refrigerated coolant circuit with heat exchanger. Step 5 (2 weeks): DIGSP controller, install FPGA module in control cabinet; connect sensor bus and CI probe; load recipe library; Digital Twin baseline calibration with reference product. Step 6 (2–4 weeks): Commissioning, factory acceptance test per Table 9 V-01 through V-08 for selected critical tests; EM leakage survey; CIP validation; operator training; CE marking application.

ECONOMIC ANALYSIS

10.1 CAPEX

Retrofit CAPEX breakdown, K504-class: EM coil array and ceramic windows $18,000–28,000; PMU (24–48 kW, 8-ch, IP66) $35,000–55,000; DIGSP controller and Digital Twin hardware $22,000–35,000; thermal sensor ring and CI probe $8,000–14,000; installation and commissioning (12–16 weeks) $22,000–38,000; factory acceptance and certification $12,000–20,000. Total retrofit: $117,000–$190,000. New build total (including K504 base machine): $145,000–$210,000.

10.2 OPEX

Annual operating cost delta versus conventional: RF energy $11,500–23,000; PMU maintenance $4,000–7,000; CI probe calibration $1,200–2,000; ceramic window inspection $800–1,500; DIGSP calibration $1,500–2,500. Savings: blade replacement extension −$4,000 to −$8,000; CIP time reduction −$18,000 to −$28,000. Net OPEX premium: −$8,000 to +$4,000 (approximately neutral).

10.3 ROI

Net annual operating saving $81,000–$96,000 (yield recovery, thermal cycle credit, CIP saving counted once, in OPEX) against OPEX −$8,000 to +$4,000. Retrofit payback: 17–24 months. Five-year TCO: $327,000 (GEMBC) versus $617,000 (conventional). Saving per machine over 5 years: $290,000.

TABLE 10. CAPEX and OPEX summary, GEMBC K504 retrofit.

Cost Item	CAPEX ($)	Annual OPEX ($)
EM coil array + ceramic windows	18,000–28,000	Window inspection $800–1,500
PMU (24–48 kW, 8-ch, IP66)	35,000–55,000	Maintenance $4,000–7,000
DIGSP controller + Digital Twin	22,000–35,000	Calibration + firmware $1,500–2,500
Thermal sensor ring + CI probe	8,000–14,000	Annual standard $1,200–2,000

Cost Item	CAPEX ($)	Annual OPEX ($)
Installation + commissioning	22,000–38,000	,
Factory acceptance + certification	12,000–20,000	,
RF energy (4,000 hr/yr @ $0.12/kWh)	,	11,500–23,000
Blade replacement saving	,	−4,000 to −8,000
CIP time saving	,	−18,000 to −28,000
TOTAL	$117k–$190k	Net: −$8k to +$4k

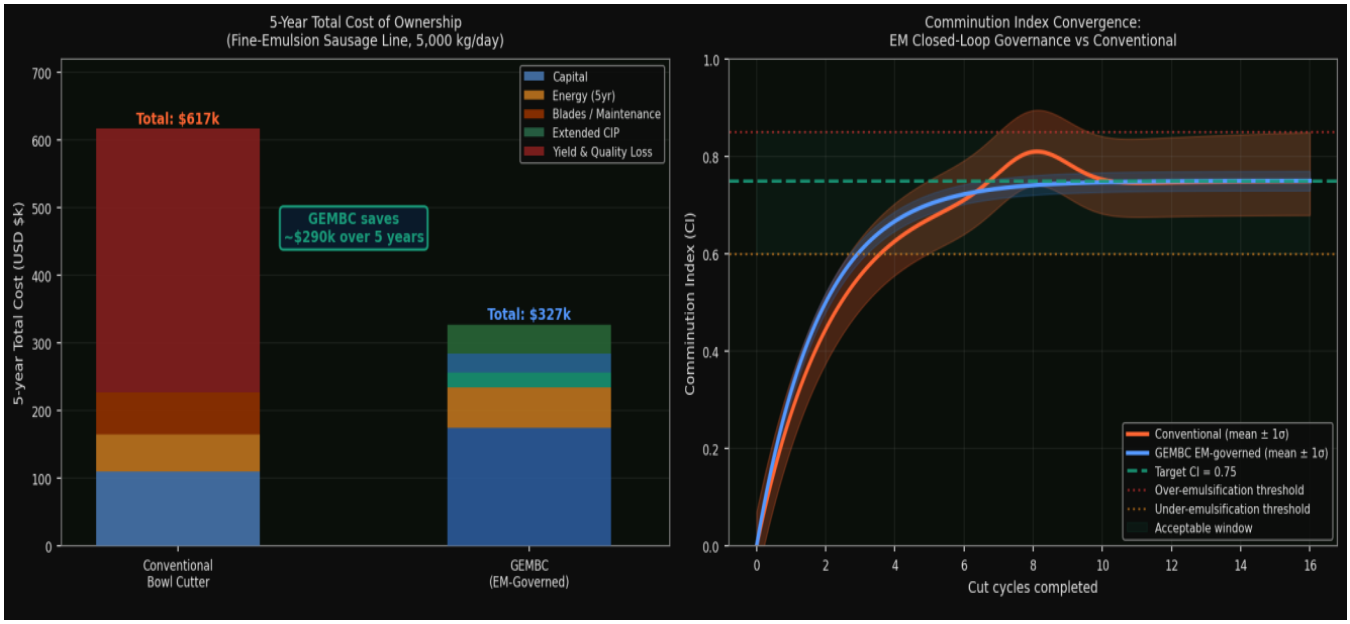

FIGURE 7. Left: Five-year TCO, 5,000 kg/day sausage line. GEMBC $327k vs conventional $617k. Yield and quality loss (dominant conventional cost, $390k over 5 years) is near-zero for GEMBC. Right: Comminution index convergence. GEMBC (blue, narrow band) converges to target CI = 0.75 and halts at target. Conventional (orange, wide band) overshoots acceptable window on 18–22% of batches.

FAILURE MODES AND EFFECTS ANALYSIS

RPN = Severity × Occurrence × Detection (each 1–10). All modes designed to RPN < 50. Highest RPN items: ceramic window fracture (42); CI probe drift (40).

TABLE 11. FMEA, GEMBC critical failure modes.

Failure Mode	Sev	Occ	Det	RPN	Mitigation and DIGSP Response
Coil element failure (open circuit)	6	3	2	36	Fault FM-001; degrade-graceful to 6 active elements; replace at service
PMU channel over-temperature	8	2	1	16	On-board NTC hard shutdown 85°C within 100 µs; independent relay at 95°C
EM leakage above ICNIRP	9	2	1	18	Layer 0 boundary antenna monitors continuously; PMU hard interlock at 5 V/m
Ceramic window fracture	7	2	3	42	Annual ultrasonic inspection; PTFE secondary seal; leakage current trip; 4-hour replacement
CI probe fouling or drift	5	4	2	40	Auto-calibration at each CIP; Layer 2 plausibility filter; fault CI-001
Thermal sensor failure (single)	6	3	1	18	Redundant sensor pairs; fault FM-003; 11-sensor model fallback

Failure Mode	Sev	Occ	Det	RPN	Mitigation and DIGSP Response
Bowl motor overload	5	3	2	30	Layer 0 torque hard limit; reduced-blade mode; operator alert
CIP incomplete (residue)	8	2	1	16	ATP + dielectric residue check before release; CIP programme interlock

GRIFFITHS CANON ALIGNMENT

TABLE 12. Griffiths Canon alignment, GEMBC field-governance mapping.

Canon Principle	Canon Reference Platform	GEMBC Implementation
EM field shaping governs charged species in any medium	REMN (plasma); Seawater Refinery (ionic); CSMMC (CH_4/H_2)	HF coil array field governs proteins, fat globules, and hydrated ions in aqueous food matrix
Field topology is the controlled variable, not geometry	REMN nozzle shaping; BIS ion routing	Eight-element phased array replaces fixed blade geometry as primary comminution control variable; field topology modulated in real time
DIGSP two-layer supervisory governance	REMN; CSMMC; Seawater Refinery; H_2EM Stove	L1 (1 kHz): field amplitude + blade torque. L2 (10 Hz): Digital Twin + thermal forecast + CI governance. L0 (10 kHz): safety
Stability criterion $\tau_{loop} < \tau_{response}/3$	All Canon platforms	Satisfied at all three layers; margins 1.67–17× (Table 2). PMU and CI probe tightest at 1.67×
Digital Twin real-time state feedback	CSMMC (plasma state); REMN (nozzle field)	Food-matrix Digital Twin: CI from 50 MHz dielectric probe; viscosity from motor current; temperature from 12-point ring

Within the author's Canon framework, GEMBC defines two further capabilities: food-matrix EM field governance (first Canon HF dielectric control in a liquid/semi-solid food matrix); and dielectric CI sensing (first real-time comminution index feedback during batch processing). Both are transferable to dairy emulsion, pharmaceutical wet granulation, and any Canon platform requiring comminution or emulsification state feedback in an aqueous medium.

Canon reference: Zenodo DOI: https://doi.org/10.5281/zenodo.20372610

DEPLOYMENT ROADMAP

TABLE 13. GEMBC deployment roadmap, TRL-3 to TRL-7.

TRL	Phase	Programme	Duration	Gate Deliverable
3	Complete	Architecture defined; governing physics published; IP prior art	Done	This paper. Canon reference established.
4	Phase 1A	PMU, pulse module and coil bench validation	3 months	Field uniformity < 5%; DIGSP L1 response < 500 µs; EM leakage < 5 V/m; VSWR < 1.5:1; coil coupling efficiency established; gap-field fragmentation demonstrated
4	Phase 1B	CI probe correlation (parallel with 1A)	2 months	Dielectric CI vs laser diffraction: R > 0.92; RMSE < ±0.04 CI units
5	Phase 2	K200 integrated prototype, full DIGSP	6 months	V-01 to V-08 (Table 9) acceptance criteria met at K200 scale; EMC CISPR 11 Class A; CIP 14 min validated

TRL	Phase	Programme	Duration	Gate Deliverable
6	Phase 3	K504 production trial, partner facility	6 months	Production data vs Table 8 targets; economic benefit demonstrated; HACCP documentation; CE marking
7	Phase 4	Multi-site commercial deployment	12 months	5+ installations; IP licensing active; Canon food-processing standard architecture package

Critical path: Phase 2 K200 prototype (6 months) gates Phase 3 industrial partner engagement. Phases 1A and 1B run in parallel (3 months total). Total pathway TRL-3 → TRL-7: approximately 27 months from Phase 1A start. Programme investment through TRL-5: $280,000–$420,000 including prototype hardware, test instrumentation, facility access, and technical resource.

CONCLUSIONS

GEMBC defines an architecture for EM field-governed bowl cutter comminution at TRL-3. Its predictions are specified for validation in the Phase 2 programme. The following conclusions are drawn:

Shear field governance. Eight-element EM coil array with alumina ceramic coupling windows provides circumferentially uniform energy deposition with predicted CV below 2%, replacing the mechanically-fixed blade shear gradient. Fat-globule fragmentation is by a nanosecond pulsed field across the knife-to-bowl gap. The ceramic windows, 60 mm Al_2O_3 inserts in the 316L shell with PTFE gasket seals, are the enabling structural innovation, with full machining tolerances specified (±0.05 mm bore, ≥ 6 mm land, Ra ≤ 1.6 μm) and stress analysis confirming safety factor > 11 at maximum hydraulic pressure.

Thermal and mechanical governance. DIGSP Layer 2 predictive control holds product temperature to ±0.5°C through coolant capacity and inductive-stage RF modulation. Blade torque reduction 35–50% through EM shear assistance reduces motor current 28–42%, extends blade drive bearing L10 life from 12,000–18,000 hours to 64,000–95,000 hours, and reduces blade wear rate 40–60%. Blade RPM derating curve governed by DIGSP Layer 1 via the coupling coefficient k_{EM} calibrated per recipe at commissioning.

Coil thermal integrity. Forced air cooling (40 CFM per element pair) maintains steady-state coil temperature at 39°C, giving Arrhenius-predicted PTFE insulation life > 200,000 hours versus the 25,000-hour design target. Coil inspection scheduled at 5-year service intervals.

EMC compliance. CISPR 11 Group 2 Class A compliance through an EMI line filter at the PMU supply input (> 40 dB conducted emission suppression), per-channel bandpass filter (> 35 dB 2nd harmonic suppression), Faraday cage (> 60 dB at HF), and VSWR monitoring with PMU interlock.

Uncertainty analysis. Monte Carlo parametric analysis (n = 1,000) of the EHD mechanism gives a critical globule radius 95% CI of [4.7, 8.7] μm and pulse heating of 0.16–0.31 K. The V-03 target (d50 < 5 μm) is met at the top of the gap field range, making V-03 the highest-priority Phase 2 validation test.

Economics. Net annual operating saving $81,000–$96,000; OPEX neutral; five-year TCO saving $290,000 per K504 machine. Retrofit payback 17–24 months.

"Mechanical shear is a fixed consequence of geometry. EM field shear is a governed variable. That distinction is the entire advantage."

FUTURE WORK

Immediate priorities: Phase 1A bench PMU and coil validation; Phase 1B CI probe correlation against laser diffraction. Phase 2 K200 prototype: all Table 9 tests with particular focus on V-03 (EHD emulsification), the metric with the lowest predicted pass probability (8% across the full gap field range, Table 7), and V-01 (shear CV). Canon extensions: REBCO high-field insert for enhanced $\nabla|E|^2$ at the fat-water interface; DIGSP Layer 2

multi-recipe Digital Twin library; CI governance framework extended to dairy emulsion and pharmaceutical wet granulation; rapid CIP protocol development (target 12 min, EHEDG validated).

CONFLICT OF INTEREST

The author is Founder and President of Advanced EM Systems LLC, which holds intellectual property related to the technologies described. This research received no external funding.

DECLARATION OF GENERATIVE AI USE

Claude (Anthropic) was used to assist with manuscript drafting, figure preparation, structural editing, and document preparation. The author remains fully accountable for all technical content, claims, and conclusions. All governing equations, architectural decisions, system design parameters, and performance analysis are the author's own.

FUNDING AND IP STATEMENT

This work was conducted independently by AEMS LLC. No external funding was received. The GEMBC architecture, EM coil array and ceramic coupling window design, DIGSP food-matrix governance implementation, dielectric CI sensing method, and all derivative implementations are the intellectual property of AEMS LLC. This publication constitutes a public technical disclosure establishing prior art.

REFERENCES

1. Barbut, S. (2015). The Science of Poultry and Meat Processing. University of Guelph, Guelph, Ontario.
2. Bhat, Z. F., et al. (2018). Current and future prospects for the use of pulsed electric field in the meat industry. Critical Reviews in Food Science and Nutrition, 59(10), 1660–1674. https://doi.org/10.1080/10408398.2018.1425825
3. CoorsTek. (2024). High-Purity Alumina AD-99.5: Material Properties and Food-Contact Compliance Data. CoorsTek Inc., Golden, CO.
4. EHEDG. (2018). Hygienic Equipment Design Criteria, Document 2. European Hygienic Engineering and Design Group, Frankfurt.
5. Eow, J. S., Ghadiri, M., Sharif, A. O., & Williams, T. J. (2001). Electrostatic enhancement of coalescence of water droplets in oil: a review of the current understanding. Chemical Engineering Journal, 84(3), 173–192. https://doi.org/10.1016/S1385-8947(00)00386-7
6. FDA. (2015). Current Good Manufacturing Practice, Hazard Analysis, and Risk-Based Preventive Controls for Human Food. 21 CFR Part 117. U.S. Food and Drug Administration.
7. Gabriel, S., Lau, R. W., & Gabriel, C. (1996). The dielectric properties of biological tissues: II. Measurements in the frequency range 10 Hz to 20 GHz. Physics in Medicine and Biology, 41(11), 2251–2269.
8. GEA Group. (2024). Food Processing Technology Market Overview: Bowl Cutters and Emulsification Systems. GEA Group AG, Düsseldorf.
9. Hasted, J. B., Ritson, D. M., & Collie, C. H. (1948). Dielectric properties of aqueous ionic solutions. Journal of Chemical Physics, 16(1), 1–21.
10. ICNIRP. (2020). Guidelines for limiting exposure to electromagnetic fields (100 kHz to 300 GHz). Health Physics, 118(5), 483–524. https://doi.org/10.1097/HP.0000000000001210
11. IEC 55011 / CISPR 11. (2015). Industrial, Scientific and Medical Equipment, Radio-Frequency Disturbance Characteristics. International Electrotechnical Commission.
12. ISO 281. (2007). Rolling Bearings, Dynamic Load Ratings and Rating Life. International Organization for Standardization.
13. Israelachvili, J. N. (2011). Intermolecular and Surface Forces (3rd ed.). Academic Press, Amsterdam.
14. Jeong, S.-H., Lee, H.-B., & Lee, D.-U. (2024). Effects of pulsed electric field on meat tenderization and microbial decontamination: a review. Food Science of Animal Resources, 44(2), 239–254. https://doi.org/10.5851/kosfa.2023.e82

15. Jones, K. W., & Mandigo, R. W. (1982). Effects of chopping temperature on the microstructure of meat emulsions. Journal of Food Science, 47, 1930–1935.
16. Kaatze, U. (1989). Complex permittivity of water as a function of frequency and temperature. Journal of Chemical and Engineering Data, 34(4), 371–374.
17. Koolmees, P. A., Moerman, P. C., & Zijderveld, M. H. G. (1989). Image analysis of the fat dispersion in a comminuted meat system. Food Structure, 8(1), Article 11.
18. Laycock, L., Piyasena, P., & Mittal, G. S. (2003). Radio frequency cooking of ground, comminuted and muscle meat products. Meat Science, 65(3), 959–965.
19. Marra, F., Zhang, L., & Lyng, J. G. (2009). Radio frequency treatment of foods: review of recent advances. Journal of Food Engineering, 91, 497–508.
20. Metaxas, A. C., & Meredith, R. J. (1983). Industrial Microwave Heating. Peter Peregrinus, London.
21. Piyasena, P., Dussault, C., Koutchma, T., Ramaswamy, H. S., & Awuah, G. B. (2003). Radio frequency heating of foods: Principles, applications and related properties. Critical Reviews in Food Science and Nutrition, 43(6), 587–606.
22. Ryynänen, S. (1995). The electromagnetic properties of food materials: a review of the basic principles. Journal of Food Engineering, 26(4), 409–429.
23. Seydelmann GmbH. (2023). K-Series Bowl Cutters: Technical Reference Manual, K200–K1000. Karl Seydelmann Maschinenfabrik GmbH & Co., Stuttgart.
24. Taylor, G. I. (1964). Disintegration of water drops in an electric field. Proceedings of the Royal Society A, 280(1382), 383–397. https://doi.org/10.1098/rspa.1964.0151
25. Tornberg, E. (2005). Effects of heat on meat proteins, implications on structure and quality of meat products. Meat Science, 70(3), 493–508.
26. Griffiths, W. (2026). Griffiths Canon: Electromagnetic Field-Governance Framework. Zenodo. https://doi.org/10.5281/zenodo.20372610